06

Brittle fracture of a conductor in a strong pulsed magnetic field

© P.A. Russkikh, G.Sh. Boltachev, S.N. Paranin

Institute of Electrophysics, Ural Branch, Russian Academy of Sciences,
Yekaterinburg, Russia
e-mail: russkikh_p@inbox.ru

Received November 9, 2022
Revised March 1, 2023
Accepted March 2, 2023

The main factors resulting in conductor failure under the action of a strong pulsed magnetic field are analyzed. The theoretical model describes the geometry of a cylindrical thick-walled solenoid and considers magnetic field diffusion, ohmic heating of the material and mechanical stresses arising in it. The magnetic field amplitude at which induced stresses in the material reach the von Mises yield criterion is used as the Bth threshold field separating the areas of safe (non-destructive) and dangerous fields. In the case of an initially uniform material, the maximum heating temperature corresponding to this limit, which predetermines the thermomechanical stress, has been derived analytically. In the general case, based on the analysis of the calculated threshold field, the influence of various parameters (magnetic pulse characteristics, elastic moduli of the material, etc.) on the conductor resistance in the pulsed magnetic field is studied and ways of increasing the threshold field are proposed, in particular, by using different spatial profiles of the initial resistivity. It is shown that in comparison with a uniform material, a modified layer with increased resistivity formed on the surface allows to significantly increase the amplitude of the magnetic pulse withstood by the material without fracture.

Keywords: Magnetic field diffusion, plastic deformation, thermomechanical stress, yield strength, von Mises yield criterion.

DOI: 10.21883/TP.2023.05.56067.243-22

Introduction

Currently, highly promising methods of magnetic pulse processing of materials attract the increased attention of many researchers. Technologies based on these methods are used for experiments on high-speed uniaxial stretching [1], compression of nanoscale powders [2,3], deformation of conductive shells [4], creation of a strong bond between dissimilar materials [5,6] and much more. One of the limitations for the widespread use of such technologies is the low lifespan of inductor systems that generate pulsed magnetic fields. At the moment, it amounts to dozens of pulses with a magnetic field amplitude of about 50 T and a pulse duration of the order of units of dozens of microseconds. The reason for the short service life is the rather rapid cracking of the working surface of the conductive material (the inner surface of the inductor, or the surface of the magnetic flux concentrator) [7,8]. Cracks are mainly caused by presence of strong thermomechanical stresses due to rapid, almost adiabatic, ohmic heating of the conductive material. Further operation of the inductor (concentrator) with incipient cracks on the surface leads to their rapid growth from -for „saw effect“ [8,9] and, ultimately, to the destruction of the material.

Cracks are initiated on the initially smooth surface of the conductor through the mechanism of low-cycle fatigue in case of a material with some plasticity resource [10–14]. In this case, exceeding the yield strength corresponding to a certain threshold amplitude of the magnetic field B_{th} during the first pulse is not a prerequisite for further destruction. Minor plastic deformation, occurring at the ohmic heating stage, during subsequent cooling inevitably leads to the appearance of residual elastic stresses stretching the surface in tangential directions. Such a material turns out to be „prepared“ for subsequent magnetic field pulses and can withstand them without re-reaching the yield strength level. The low-cycle fatigue mechanism will be triggered if the material reaches the yield threshold [15] twice during the first pulse: during ohmic heating and subsequent cooling. At the same time, even a single achievement of the yield strength at the very first heating can be destructive in the case of a relatively brittle material that does not have a sufficient plasticity resource [16]. This (*brittle*) destruction of the conductive material is the subject of study in this paper. The tendency for brittle fracturing will be assessed based on the yield strength in the form of Mises stresses. Therefore, in the future we will use the minimum amplitude of the magnetic field on the surface of the conductor as a criterion of destruction, at which the induced thermomechanical stresses in the material satisfy the Mises plasticity condition, i.e., the material reaches the yield point. We will call this minimum amplitude the threshold field B_{th}, separating the areas of safe (non-destructive) and dangerous fields.

Various approaches can be applied to increase the lifespan of inductor systems: optimization of the shape of the external magnetic pulse $B_0(t)$ [17,18], the use of a diamagnetic shield with inertial confinement [19], etc. However, the most attractive method is the one discussed in [19,20], which consists in creating a gradient resistance profile in

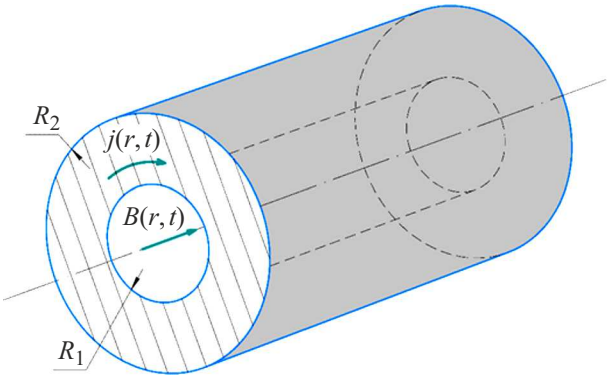

Figure 1. The geometry of a model conductor (hollow cylinder) simulating the inner region of an inductor or a magnetic flux concentrator.

a conductive material. The main current and heating in a material with a specific electrical resistance decreasing from the surface are shifted deep into the material [17,18,21], which can noticeably increase its resistance in pulsed fields. It is worth noting that the studies of [17,18,21] did not take into account the change in electrical resistance during heating. This factor becomes decisive for strong magnetic fields with an amplitude of about 30 T or more, in particular, it is due to the well-known „peak effect“ [22,23].

Thus, in this paper we investigate the effect of a strong, about 30 T, pulsed magnetic field on a brittle conductive material in the form of a hollow cylinder with both a spatially homogeneous initial resistivity and with different profiles of initial electrical resistance on the inner (working) surface. The cylindrical geometry of the conductor implies the use of the results obtained to increase the lifespan of inductor systems. The amplitude of the fields studied in this work is tens of teslas, which, on the one hand, makes it possible to neglect the effects of magnetic hysteresis observed in weak fields [24–27], and on the other hand, to avoid the melting and explosion of the conductor occurring in super-strong magnetic fields (more than 100 T), which requires the use of wide-range equations of state of matter [22,28–31].

1. Theoretical model

We will consider the hollow cylindrical conductor shown in Fig. 1. The natural „weak point“ of such a conductor is the inner surface near the sharp end edge. In practice, this edge is smoothed to level out undesirable edge effects in the manufacture of magnetic flux concentrators [7]. Experimental data on the destruction of such concentrators show that the nucleation of cracks on their surface can occur in the middle part of the concentrator [7], i.e. it is not related to the geometry of the end part. Therefore, we will consider the conducting cylinder to be sufficiently extended to simplify the theoretical model, neglecting the edge effects of [32,33]. In such a statement, using a cylindrical coordinate system (r, φ, z) with z- axis aligned with the axis of the conductor, it can be argued that the displacement of the material $\mathbf{w}$ is possible only in the radial direction, i.e. $\mathbf{w} = (w, 0, 0)$, magnetic field induction $\mathbf{B}$ has only z-component, i.e. $\mathbf{B} = (0, 0, B)$, etc. In this case, all the desired functions depend on the radius r and the time t.

The spatial distributions of the magnetic field $B(r, t)$ and the current density $j(r, t)$ are determined by the well-known magnetic diffusion equation [22]:

$$\frac{\mu}{\rho_e}\frac{\partial B}{\partial t} = \frac{\partial^2 B}{\partial r^2} + \left(\frac{1}{r} + \frac{1}{\rho_e}\frac{\partial \rho_e}{\partial r}\right)\frac{\partial B}{\partial r},$$

$$j(r,t) = -\frac{1}{\mu}\frac{\partial B}{\partial r}, \qquad (1)$$

where $\mu = 4\pi \cdot 10^{-7}$ H/m is a magnetic constant. The initial condition for the differential equation (1) is the absence of a magnetic field in the conductor at the moment $t = 0$. We will use the absence of a magnetic field at the outer boundary of the conducting cylinder ($B = 0$ at $r = R_2$) and the pulse of the magnetic field in the inner cavity as a boundary condition, i.e. at the boundary of $r = R_1$, in the form of four periods of a decaying sine wave:

$$B_0(t) = B_m \exp\left(-\frac{t}{T_e}\right)\sin\left(\frac{2\pi t}{T_s}\right), \quad 0 < t < 4T_s, \qquad (2)$$

with parameters $T_e = 20\,\mu$s and $T_s = 24\,\mu$s, which corresponds to typical magnetic field pulses in experiments [7,34]. The electrical resistivity ρ_e of the material was set as follows:

$$\rho_e(r,t) = \rho_e^*[\gamma_e(r) + k_\rho T(r,t)], \qquad (3)$$

where ρ_e^* is the initial electrical resistance (before heating) of the material away from the modified surface, multiplier k_ρ is the temperature coefficient of resistance, T is the temperature increment relative to the initial (room) value. The dependence $\gamma_e(r)$, which determines the initial electrical resistance in the modified layer, was set as [15]:

$$\gamma_e(r) = 1 + \gamma_0 \exp[-(x/x_c)^{N_\gamma}], \quad x = r - R_1, \qquad (4)$$

where γ_0 is the „amplitude“ of the modifications, x_c is the effective depth of the modified layer and $N_\gamma \geq 1$ is the parameter characterizing the sharpness of the transition at the boundary of the modified layer. The larger the N_γ, the smaller the transition region between the surface (near $r = R_1$) highly resistive (at $\gamma_0 > 0$) layer and the inner region of the conductor. For a sharp ($N_\gamma \to \infty$) step profile $\gamma_e = 1 + \gamma_0$ at $x < x_c$ and $\gamma_e = 1$ at $x > x_c$. The minimum value $N_\gamma = 1$ corresponds to the smoothest, exponential profile of the initial resistivity.

The temperature increment T is described by the thermal conductivity equation as

$$c\frac{\partial T}{\partial t} = \frac{\lambda}{r}\frac{\partial}{\partial r}\left(r\frac{\partial T}{\partial r}\right) + \rho_e j^2 + \sigma^{ij}\frac{\partial \varepsilon_{ij}}{\partial t}, \qquad (5)$$

where c is the volumetric heat capacity, λ is the thermal conductivity coefficient, the second term on the right describes ohmic heating, and the third term is the mechanical work (σ^{ij} and ε_{ij} are the stress and strain tensors, respectively). The initial condition for equation (5): $T(r) = 0$ at $t = 0$. The adiabaticity of the inner and outer surfaces was used as boundary conditions, i.e. $\partial T/\partial r = 0$ with $r = R_1$ and $r = R_2$.

The occurrence of mechanical stresses in the thickness of the conductive material when current flows through it $j(r, t)$ is caused, in -first, by the action of the volumetric Ampere force $f_a = [\mathbf{j} \times \mathbf{B}]$, for the radial component of which we have

$$f_a = -\frac{1}{\mu} B \frac{\partial B}{\partial r},$$

and, in-second, thermoelastic stresses, which we will describe in the framework of the linear elastic body model [35,36]:

$$\sigma_i = \frac{E\nu}{(1-2\nu)(1+\nu)} tr(\varepsilon_{ij}) + \frac{E}{(1+\nu)} \varepsilon_i - \frac{E}{(1-2\nu)} \beta_V T,$$

$$(i = r, \varphi, z), \qquad (6)$$

where β_V is the coefficient of linear thermal expansion, E is the Young's modulus, ν is the Poisson's ratio. The problem of the distribution of mechanical stresses and deformations is analyzed in a quasi-static approximation that corresponds to the condition of mechanical equilibrium [36]:

$$\frac{\partial \sigma_r}{\partial r} + \frac{\sigma_r - \sigma_\varphi}{r} = \frac{1}{\mu} B \frac{\partial B}{\partial r}. \qquad (7)$$

The following was used as boundary conditions for the mechanical problem (6), (7): absence of radial stresses at the inner boundary $\sigma_r(R_1) = 0$ [12] and absence of displacements at the outer boundary $w(R_2) = 0$. The Mises yield criterion is used to determine the ultimate elastic stresses and deformations [36]

$$(\sigma_r - \sigma_\varphi)^2 + (\sigma_r - \sigma_z)^2 + (\sigma_\varphi - \sigma_z)^2 = 2\sigma_s^2,$$

$$\sigma_s(T) = \sigma_{s,0} \left(1 - \frac{T}{T_{melt}}\right), \qquad (8)$$

where σ_s is the yield strength of the material under uniaxial tension, approximated by linear dependence on temperature, T_{melt} is the melting point. The values of $\sigma_{s,0} = 1\,\text{GPa}$ and $T_{melt} = 1400^\circ\text{C}$, corresponding to the steel 30XGSA [37], were used for calculations.

The results obtained within the framework of the formulated theoretical model for a cylindrical conductor with radii $R_1 = 5\,\text{mm}$, $R_2 = 13\,\text{mm}$ and parameters corresponding to steel 30XGSA [37] are provided below: $\rho_e^* = 42 \cdot 10^{-8}\,\Omega \cdot \text{m}$, $c = 461\,\text{J/(kg·K)}$, $k_\rho = 1.38 \cdot 10^{-3}\,\text{K}^{-1}$, $\lambda = 39\,\text{W/(m·K)}$, $E = 205\,\text{GPa}$, $\nu = 0.3$, $\beta_V = 13 \cdot 10^{-6}\,\text{K}^{-1}$.

2. Results and discussion

2.1. Homogeneous material: the effect of various parameters on the threshold field value

We investigate in this section the effect of a pulsed magnetic field on a homogeneous conductive material, i.e. when in (4) „the amplitude" of the modification $\gamma_0 = 0$, and at the initial moment the resistivity $\rho_e = \rho_e^*$ in the entire conductor. As noted in the introduction, one of the ways to increase the resource of the inductor system is to optimize the shape of the external magnetic pulse $B_0(t)$ [17,18]. This possibility can be realized by varying the parameters T_e and T_s of the pulse (2) within the framework of the theoretical model formulated in the previous section. These parameters are determined by the resistance and inductance of the inductor system, and also the capacity of the capacitor bank used in real experimental setups [7,34].

Figure 2 shows the dependences of the calculated threshold field B_{th} on the value T_e at a fixed value $T_s = 24\,\mu\text{s}$ and, conversely, on the value T_s at a fixed $T_e = 20\,\mu\text{s}$. Similar dependencies obtained in the plane geometry [15], i.e. corresponding to the limit $R_1 \to \infty$ are provided there for comparison. The dependence $B_{th}(T_e)$ shows that it is preferable to use a circuit with rapid attenuation (small values T_e), i.e. with relatively high values of electrical resistance to increase the resource of the inductor system. This is explained by the fact that the main („working") half-period, which creates the main maximum of the magnetic field, is the first half-period, at $t < T_s/2$, while subsequent electrical oscillations lead only to additional („parasitic") heating of the conductive material. Thus, it would be most promising to use a circuit that completely cuts off the flow of current through the inductor at the end of the first half-cycle of oscillations [15].

The dependence $B_{th}(T_s)$, shown in Fig. 2 on the right, shows that the threshold field increases markedly when using relatively long pulses (2), the period T_s of which exceeds the characteristic attenuation time T_e. In - of the first, this is again due to the effective „quenching of " subsequent („parasitic") oscillations at $T_s > T_e$. In addition to this factor, an increase in T_s leads to an increase in the thickness of the skin-layer, $\delta = \sqrt{\rho_e T_s/(\pi\mu_0)}$, which reduces the sharp localization of surface heat generation and distributes heat more evenly over the conductive material. This, in turn, reduces the heating temperature on the surface, which makes it possible to realize a higher magnetic field without the threat of destruction.

It can also be noted here that in flat geometry, unlike cylindrical, the material demonstrates greater durability, i.e., large values of threshold fields B_{th}. The latter is attributable, -firstly, to a higher concentration of current in a cylindrical conductor in the region of small radii [22], which is mathematically related to the presence of a term proportional to r^{-1} in (1), and, secondly, to-, with an additional source of stress growth when heating curved layers — a term proportional to r^{-1} in (7).

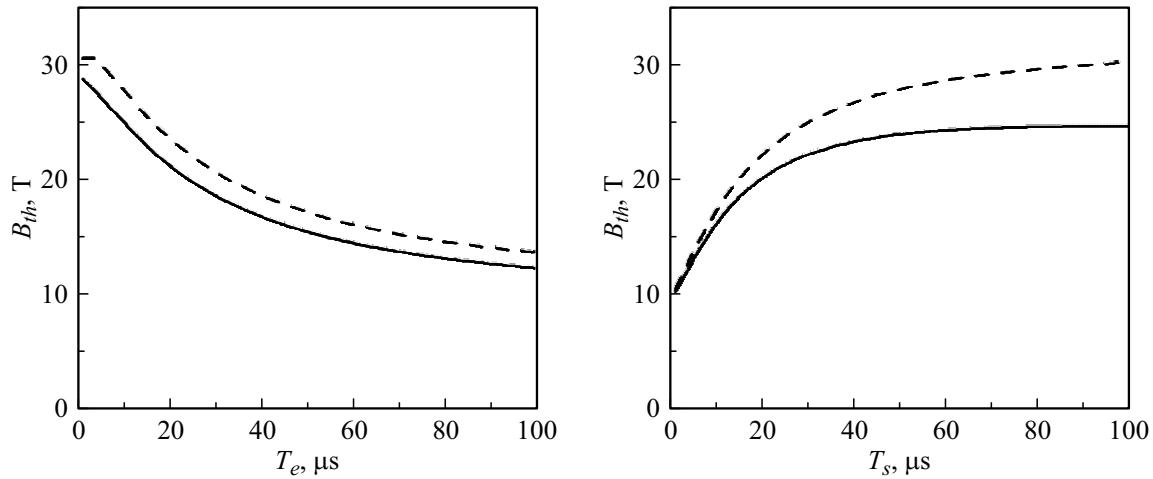

Figure 2. Threshold field dependencies B_{th} for a steel cylindrical conductor ($R_1 = 5$ mm) at a pulse in the form of (2) from parameter T_e at fixed $T_s = 24\,\mu$s (left) and from parameter T_s at fixed $T_e = 20\,\mu$s (right). Dashed lines — flat geometry ($R_1 \to \infty$).

Values of the influence coefficient (9) for heat capacity c, thermal expansion coefficient β_V, Young's modulus E, Poisson's ratio ν and parameter $\sigma_{s,0}$

χ	c	β_V	E	ν	$\sigma_{s,0}$
P_χ	0.49	−0.44	−0.44	−0.23	0.44

Next, we will analyze the impact of various individual properties of the material (heat capacity, Young's modulus, etc., etc.) on its resistance to a magnetic pulse (2) with fixed parameters $T_e = 20\,\mu$s and $T_s = 24\,\mu$s. Of course, it is difficult to change individual properties of a given material (for example, by doping), but such an analysis can be useful for selecting the starting material at the stage of manufacturing an inductor system. We will use

$$P_\chi = \frac{\chi}{B_{th}} \left(\frac{\partial B_{th}}{\partial \chi} \right). \qquad (9)$$

as a value characterizing the impact of a certain parameter (denoted as χ) on the resistance of the conductive material

The table shows the values of the influence coefficients P_χ for parameters such as heat capacity c, thermal expansion coefficient β_V, Young's modulus E, Poisson's ratio ν and yield strength at room temperature $\sigma_{s,0}$. The dependencies $B_{th}(\chi)$ for all these parameters are close to linear within the limits of their variation characteristic of various steels [37]. We see that the heat capacity c has the greatest influence on the threshold field. Higher values of heat capacity correspond to an increase in resistance, since this reduces the heating temperature. An increase in the elastic parameters E and ν, as well as an increase in β_V, leads to an increase in thermoelastic stresses at a given heating, which reduces the threshold field. The increase in yield strength had the same effect on B_{th} as the decrease in the three previous parameters. Thus, the analysis shows that, all other things being equal (first of all, with the same specific conductivity), it is preferable to use a material with high values of heat capacity and tensile strength and low values of the coefficient of thermal expansion and elastic parameters as an inductor material.

In contrast to the individual parameters listed in the table, the change of which for a given material is difficult to implement, the resistivity of the material ρ_e^* seems to be a more convenient parameter for varying within a sufficiently wide range. Firstly-, the resistivity values are very different for different conductive materials, and -secondly, even for a given material, a sufficiently wide change in the value of ρ_e^* is possible due to doping, ionically-plasma processing, powder technologies, the use of composite (for example, bimetallic) conductive materials,

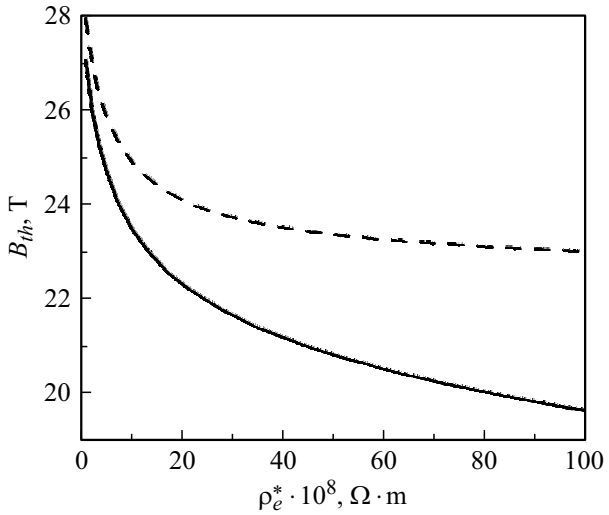

Figure 3. Dependence of the threshold field on the resistivity for a homogeneous cylindrical conductor ($R_1 = 5$ mm, solid line) and in flat geometry ($R_1 \to \infty$, dashed line).

etc., etc. [16,20,38,39]. In this regard, we will analyze the dependence of $B_{th}(\rho_e^*)$ in the range from the resistance of copper ($\rho_e^* = 1.7 \cdot 10^{-8}\,\Omega \cdot \mathrm{m}$) to the resistance of high-resistive steels ($\rho_e^* \approx 100 \cdot 10^{-8}\,\Omega \cdot \mathrm{m}$). At the same time, all other parameters of the material and the temperature dependence of the resistance, i.e., the derivative $d\rho_e/dT$, will be recorded at values corresponding to the steel 30XGSA. The dependence $B_{th}(\rho_e^*)$ obtained in this way is shown in Fig. 3. We see that an increase in the electrical conductivity of the material, i.e., a decrease in ρ_e^*, increases the threshold field values from $B_{th} \approx 16.9\,\mathrm{T}$ at $\rho_e^* = 100 \cdot 10^{-8}\,\Omega \cdot \mathrm{m}$ to $B_{th} \approx 26.4\,\mathrm{T}$ at $\rho_e^* = 1.7 \cdot 10^{-8}\,\Omega \cdot \mathrm{m}$. It is interesting to note that the threshold field increases with a decrease of ρ_e^* as shown in Fig. 4 (left) despite the higher values of the current density realized in the surface layer of a highly conductive material. The increase of current density with a decrease of ρ_e^* is caused in the first approximation by a change in the thickness of the skin-layer, $j \propto \rho_e^{-1/2}$, and, consequently, the surface heating rate ($c\partial T/\partial t$), determined by the term $\rho_e j^2$ in (5), should not depend on the resistivity of the material. In particular, with a monotonous increase in the magnetic field on the surface of the conductor $cT \approx B^2/(2\mu)$ [22,40]. In our case, the heating of a highly conductive material with $\rho_e^* = 1.7 \cdot 10^{-8}\,\Omega \cdot \mathrm{m}$ is noticeably lower than the heating of high-resistive steel for a given amplitude of the magnetic field (Fig. 4 on the right). This is attributable to the following factors.

Firstly-, the reduction of ρ_e^* with a fixed derivative $d\rho_e/dT$ enhances the nonlinear nature of magnetic diffusion. As you know [22], the characteristic field of manifestation of nonlinear effects corresponds to an increase in resistivity by 2 times. This conditional criterion is not achieved by heating a highly resistive material and is relatively quickly overcome at low values of ρ_e^*. Therefore, in a highly conductive material, we observe the formation of a so-called nonlinear diffusion wave (Fig. 4, left), which shifts the main heat release, i.e., the maximum current density, deep into the material [40.41]. This factor is attributable to a rather rapid increase of the threshold field in Fig. 3 in the region of small values ρ_e^*, observed both for a curved surface ($R_1 = 5\,\mathrm{mm}$) and in a flat limit ($R_1 \to \infty$). Secondly-, reduction of the thickness of the skin-of layer from the value of $\delta \approx 2.5\,\mathrm{mm}$ at $\rho_e^* = 100 \cdot 10^{-8}\,\Omega \cdot \mathrm{m}$ to $\delta \approx 0.3\,\mathrm{mm}$ at $\rho_e^* = 1.7 \cdot 10^{-8}\,\Omega \cdot \mathrm{m}$ noticeably enhances the role of heat exchange, which also reduces heat generation on the surface, striving to distribute it more evenly over the material. And finally, thirdly-, as already noted above, the current tends for concentrating in the area of smaller radii on a curved surface, which contributes to a stronger heating of such a surface compared to a flat boundary. The role of this factor becomes especially noticeable at large values ρ_e^*, when the thickness of the skin- of the layer becomes comparable to the radius of curvature R_1. This explains the increase of the discrepancy between the curves $B_{th}(\rho_e^*)$ in Fig. 3 for a curved and flat surface with an increase of ρ_e^*. The effect of surface curvature on the threshold field and surface heating of the conductor will be discussed in more detail in the next section.

2.2. Homogeneous material: the effect of surface curvature

The dependence $B_{th}(R_1)$ for a steel ($\rho_e^* = 42 \cdot 10^{-8}\,\Omega \cdot \mathrm{m}$) cylindrical conductor with a thickness of $R_2 - R_1 = 8\,\mathrm{mm}$ is shown in Fig. 5. The threshold field value rapidly tends to a flat limit $B_{th,\infty} \approx 23\,\mathrm{T}$ in the region of high values of the surface radius ($R_1 > \delta \approx 1.6\,\mathrm{mm}$). At the opposite limit ($R_1 \to 0$), the threshold field decreases down to zero ($B_{th} \approx B_1^{1/2}$), i.e., the resistance of the inductor (or concentrator) will decrease fairly quickly with an increase in the curvature of its working surface. The decrease of the threshold field with a decrease of R_1 is attributable to an increasingly sharp concentration of current in the surface layer, which even with a decrease in the magnetic field down to zero ensures that a sufficiently high surface heating temperature is reached (Fig. 5, right). It is the inhomogeneous heating, i.e., an increase in surface temperature, that determines the level of thermoelastic stresses in the material, and, as a consequence, the achievement of the Mises condition (8). The magnetic field at the same time acts only as a tool that provides the energy supply necessary for heating.

As shown in Fig. 5 (right), the heating temperature of the working surface T_{plast}, corresponding to the achievement of the yield strength of the material, demonstrates a non-monotonic dependence on the radius of curvature. The limit value $T_{plast,\infty}$, (for $R_1 \to \infty$), marked with a dashed line in the figure, as obtained in our previous work [15], is determined by the ratio

$$T_{plast,\infty} = \frac{1-\nu}{E\beta_V}\,\sigma_s(T_{plast,\infty}), \tag{10}$$

which in our case gives $T_{plast,\infty} \approx 221\,\mathrm{K}$. When the radius decreases R_1 , the threshold heating temperature T_{plast} first decreases, reaches a minimum ($\approx 209\,\mathrm{K}$) at $R_1 \approx 3\delta$, and then increases again to the value $T_{plast} \approx T_{plast,\infty}$ when $R_1 \to 0$. A fairly accurate analytical estimate can be derived for it despite such a rather complex nature of the dependence $T_{plast}(R_1)$. Let's show it.

The solution of a system of equations (6) and (7) for azimuthal and axial stresses σ_φ and σ_z on the working surface ($r = R_1$) has the following form in the field of elastic deformations

$$\sigma_\varphi = \frac{\nu}{(1-\nu)}\,\frac{B_0^2}{2\mu} - \frac{E}{(1-\nu)}\,\beta_V T + \frac{E}{(1+\nu)}\,\frac{2c_1}{(1-2\nu)} + \frac{R_1^2}{r^2}\,\frac{B_0^2}{2\mu},$$

$$\sigma_z = \frac{\nu}{(1-\nu)}\,\frac{B_0^2}{2\mu} - \frac{E}{(1-\nu)}\,\beta_V T + \frac{E}{(1+\nu)}\,\frac{2\nu c_1}{(1-2\nu)},$$

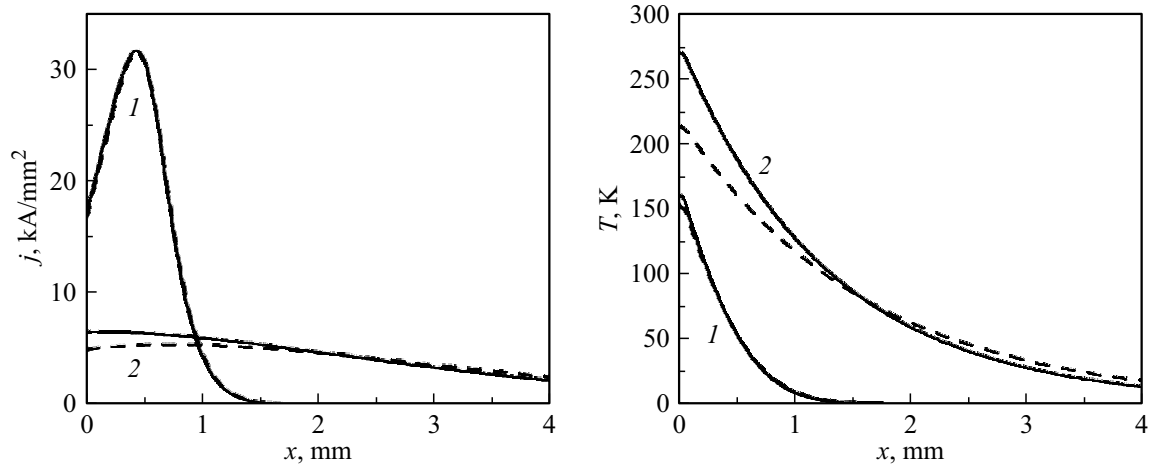

Figure 4. Radial ($x = r - R_1$) dependences of current density at the moment $t = T_s/4$ (left) and temperature at the moment of maximum surface heating (right) for a homogeneous cylindrical conductor ($\gamma_0 = 0$, $R_1 = 5$ mm) at the amplitude of the magnetic field $B_m = 30$ T and the resistivity values $\rho_e^* = 1.7 \cdot 10^{-8}\,\Omega \cdot$ m (curves *1*) and $100 \cdot 10^{-8}\,\Omega \cdot$ m (curves *2*). Dashed lines — same for flat geometry ($R_1 \to \infty$).

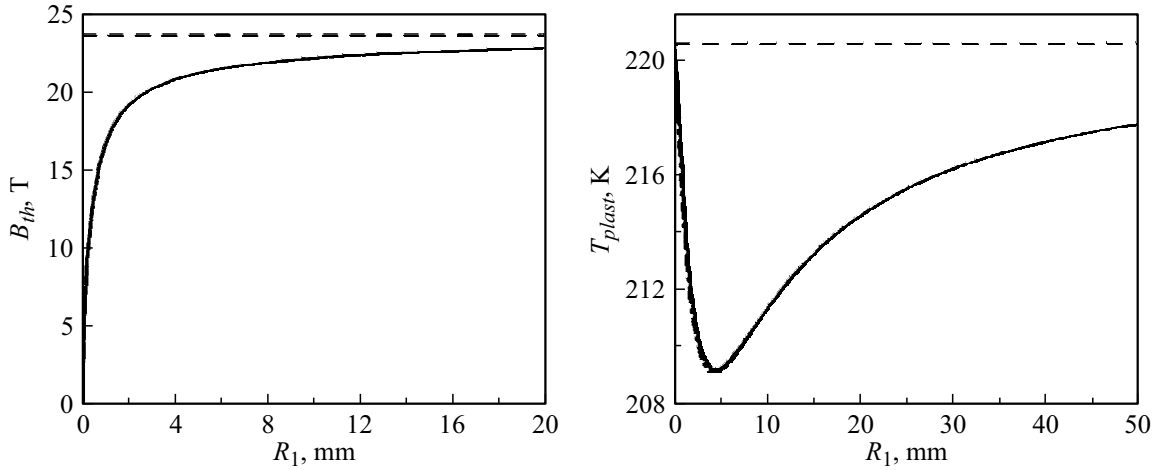

Figure 5. The dependence of the threshold field B_{th} (left) and the maximum temperature T_{plast} of heating the surface (right) corresponding to this threshold field on the inner radius R_1 of the cylindrical conductor. The dashed lines correspond to the flat limit $R_1 \to \infty$. Dashpoint curve — analytical evaluation T_{plast} (15).

$$c_1 = -\frac{1+\nu}{E}\left(\frac{1-2\nu}{1-\nu}J_B + \frac{E\beta_V J_T}{1-\nu} + \frac{B_0^2}{2\mu}R_1^2\right)\Bigg/\left(R_2^2 + \frac{R_1^2}{1-2\nu}\right),$$

$$J_B = \int_{R_1}^{R_2} \frac{B^2}{2\mu} r dr, \qquad J_T = \int_{R_1}^{R_2} T r dr.$$

Since we are interested in the moment of maximum heating, which occurs approximately at the end of the magnetic pulse, i.e. at $B_0 \approx 0$, we neglect the corresponding terms, which gives

$$\sigma_\varphi = \frac{-E}{1-\nu}\beta_V T - \beta_V J_T \frac{2E}{(1-\nu)}/[(1-2\nu)R_2^2],$$

$$\sigma_z = \frac{-E}{1-\nu}\beta_V T - \beta_V J_T \frac{2\nu E}{(1-\nu)}/[(1-2\nu)R_2^2]. \qquad (11)$$

These stresses should be substituted into the Mises criterion (8) to obtain the desired temperature T_{plast}, which on the surface $r = R_1$, due to the boundary condition $\sigma_r = 0$, takes the following form

$$\sigma_\varphi^2 - \sigma_\varphi \sigma_z + \sigma_z^2 = \sigma_s^2, \qquad (12)$$

It is easy to see that in the flat limit ($R_1, R_2 \to \infty$) we have

$$\sigma_\varphi = \sigma_z = -E\beta_V T/(1-\nu),$$

which leads to the ratio (10) when substituting in (12). At $R_1 \neq 0$, the sought temperature T_{plast} depends on the value of the integral J_T. The calculated dependence $J_T(R_1)$ is shown in Fig. 6. Due to the contraction of the current

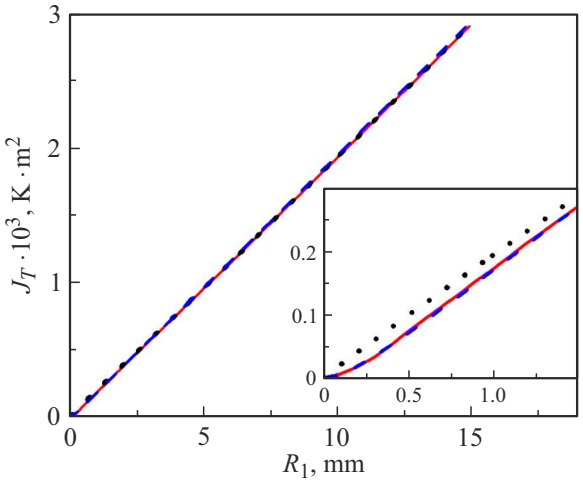

Figure 6. Integral J_T depending on the radius R_1. Solid (red) line is the numerical calculation, dotted (black) line is the analytical evaluation (14), dashed (blue) line is the result of the solution (1) using the Laplace transform. The inset shows an enlarged area of small radii R_1.

flow region to the surface $r = R_1$ in the limit $R_1 \to 0$, the integral J_T tends to zero. At the same time, the second terms on the right in equations (11) also disappear, which explains the return of the temperature T_{plast} in Figure 5 to the value $T_{plast,\infty}$ at $R_1 \to 0$.

In the general case, to obtain the dependence $J_T(R_1)$, it is required to solve a system of magnetic diffusion equations (1) and thermal conductivity (5). We neglect the impact of temperature on the value of resistivity for the possibility of an analytical solution (1). In this case, the magnetic diffusion equation (1) becomes independent and can be solved using the Laplace transform [42]. It is possible to obtain the temperature field $T(r, t)$ and the sought integral J_T using the current density determined by this solution $j(r, t)$, from the thermal conductivity equation (5) ignoring the heat exchange and mechanical work. The result of such an analysis is represented in Fig. 6 by a dashed line. We see that the result obtained using the Laplace method allows describing the dependence $J_T(R_1)$ with a sufficiently high accuracy. However, the expressions obtained using the Laplace method are rather cumbersome, so we do not provide them. Instead, we will present a much easier derivation, which allows us to obtain the integral J_T with a slightly lower, but still quite acceptable accuracy.

Figure 6 shows that with the exception of a relatively small area of radii, namely the area $R_1 < \delta \approx 1.6\,\text{mm}$, the dependence $J_T(R_1)$ is close to linear ($J_T = k_J R_1$). It is possible to obtain the proportionality coefficient k_J of this dependence by estimating the value of the integral J_T in the region of large radii R_1. In this case , the magnetic diffusion equation takes the form

$$\frac{\partial B(x,t)}{\partial t} = \frac{\rho_e}{\mu}\frac{\partial^2 B(x,t)}{\partial x^2}, \qquad (13)$$

where $x = r - R_1$. Using now instead of condition (2) stationary boundary condition

$$B(0,t) = B_m \sin\left(\frac{2\pi t}{T_s}\right),$$

it is not difficult to write the solution (13) for the so-called steady state [22]:

$$B(x,t) = B_m \exp\left(-\frac{x}{\delta}\right)\sin\left(\frac{2\pi t}{T_s} - \frac{x}{\delta}\right).$$

Substituting this solution into the thermal conductivity equation (5) and performing half-cycle integration (from $t = 0$ to $t = T_s/2$) in disregard of heat exchange and mechanical work, we obtain for the temperature field:

$$T(x) = T_0 \exp\left(-\frac{2x}{\delta}\right), \quad T_0 = \frac{\pi B_m^2}{2\mu c}.$$

Using this temperature field to estimate the desired integral J_T, in the approximations $R_1 \gg \delta$ and $R_2 - R_1 \gg \delta$ we obtain

$$J_T = \frac{1}{2} T_0 \delta R_1. \qquad (14)$$

The linear dependence $J_T(R_1)$, determined by the resulting expression, is represented in Fig. 6 by a dotted line. Substituting this dependence into equations (11) and (12), we obtain the ratios for the value of the surface temperature leading to the achievement of the yield threshold $T_0 = T_{plast}$

$$T_{plast} = \frac{1-\nu}{E\beta_V}\frac{\sigma_s(T_{plast})}{\sqrt{m^2(\nu^2-\nu+1)+m(1+\nu)+1}},$$

$$m = \frac{R_1\delta}{R_1^2 + (1-2\nu)R_2^2}, \quad \delta = \sqrt{\frac{T_s\rho_e(T_{plast})}{\pi\mu_0}}, \qquad (15)$$

where the temperature dependences of the yield strength at uniaxial tension $\sigma_s(T)$ and the resistivity $\rho_e(T)$ in our case are determined by the relations (8) and (3) respectively. It can be seen that (15) becomes an expression for the flat case (10) both for large radii R_1 and R_2, and for $R_1 \to 0$. The dependence $T_{plast}(R_1)$, defined by (15), is shown in Fig. 5 (right). It can be seen that the obtained analytical estimate agrees well with the result of direct numerical calculation over the entire range of radii R_1.

Thus, the obtained result (15) makes it possible to carry out an analytical assessment of the heating of the surface, which poses a threat of destruction for a relatively brittle initially homogeneous material due to the achievement of a critical level by thermoelastic stresses, i.e., the yield strength. An effective reduction of the surface heating of the conductor in an external pulsed magnetic field, i.e., a reduction of the threat of its destruction, can be achieved by using an initially inhomogeneous material with increased resistivity near the working surface [15,22]. The following section is devoted to the study of this possibility within the framework of modified profiles (4).

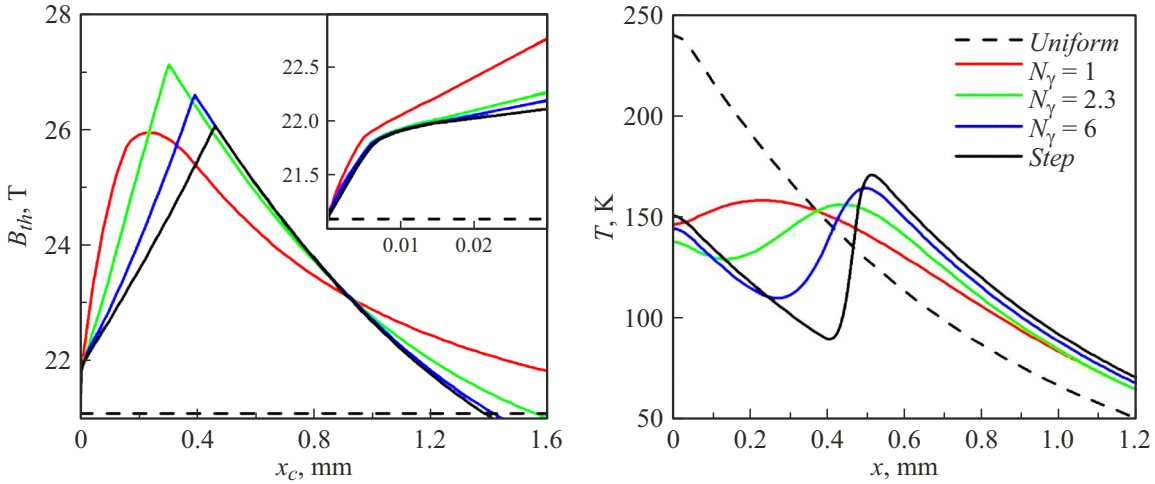

Figure 7. The dependencies of the threshold field B_{th} on „depth“ modified layer x_c at $\gamma_0 = 1.5$ for values $N_\gamma = 1.0,\ 2.3,\ 6.0$ and for a step profile are shown on the left ($N_\gamma \to \infty$). The radial ($x = r - R_1$) dependences of the maximum heating temperature of the material for the pulse (2) with $B_m = 30\,\mathrm{T}$ with the same values γ_0 and N_γ and „depth“ $x_c = x_{c,\max}$ are shown on the right. The dashed lines correspond to a homogeneous material ($\gamma_0 = 0$).

Increasing of the durability of the material due to the formation of an inhomogeneous profile of the initial resistivity

Figure 7 (left) shows the dependencies of the threshold field B_{th} on the „depth“ of the modified layer x_c for various types of modification profile (4), which correspond to certain values of the parameter N_γ from the most smooth (exponential) at $N_\gamma = 1$ to stepwise at $N_\gamma \to \infty$. As the „of the amplitude“ modification for all profiles $\gamma_e(r)$, $\gamma_0 = 1.5$ is used, i.e., in the initial (non-heated) state, the resistivity on the surface is 2.5 times greater than its value in depth: $\rho_e(R_1) = (1 + \gamma_0)\rho_e^* = 105 \cdot 10^{-8}\,\Omega \cdot \mathrm{m}$, which practically coincides with the upper limit of the resistance range of high-resistive steels, shown in Fig. 3.

Unmodified material with $\rho_e = \rho_e^* = 42 \cdot 10^{-8}\,\Omega \cdot \mathrm{m}$ has a threshold field $B_{th} \approx 21.1\,\mathrm{T}$. An increase of the resistivity of the entire material, as can be seen, in particular, in Fig. 3, reduces the threshold field to about 19.6 T. At the same time, as Figure 7 shows, an increase of the initial resistivity in a relatively small surface layer with a depth of x_c of no more than 1 mm makes it possible to significantly increase the threshold magnetic field. The dependence $B_{th}(x_c)$ demonstrates a non-monotonic character with a maximum at some, most optimal, „depth“ of the modified layer $x_c = x_{c,\max}$. The coordinates of this maximum ($x_{c,\max}$ and $B_{th,\max}$) are different for different profiles. So, for an exponential profile $x_{c,\max} \approx 0.24\,\mathrm{mm}$ and $B_{th,\max} = 25.9\,\mathrm{T}$, and for a sharp (stepped) $x_{c,\max} \approx 0.46\,\mathrm{mm}$ and $B_{th,\max} = 26.1\,\mathrm{T}$. In works [17,18] it is stated that the most advantageous resistance profile $\rho_e(x)$ is exponential ($N_\gamma = 1$). However, the analysis carried out by the authors of [17,18] did not take into account the increase in resistivity with temperature. Our calculations, taking into account this factor, show that a profile with a sharper transition corresponding to the value $N_\gamma \approx 2.3$ is most preferable for 30XGSA steel at „amplitude“ modification $\gamma_0 = 1.5$. The threshold field for this field increases to the value $B_{th,\max} = 27.1\,\mathrm{T}$, i.e., by about 28% relative to the unmodified material as shown in Fig. 7.

The radial dependences of the maximum heating $T(x)$, which is achieved, as a rule, by the end of the magnetic field pulse ($t = 4T_s$) is considered to explain the effect of the modified layer on the threshold field value and the nature of the change B_{th} with an increase of the „depth“ of this layer. These dependencies for $B_m = 30\,\mathrm{T}$, $\gamma_0 = 1.5$ with the modification thickness optimal for each profile are shown in Fig. 7 on the right. The heating of unmodified material is shown there for comparison with the same amplitude of the magnetic pulse. The increased resistivity of the surface layer shifts a significant proportion of the heating deep into the material, in the region $x > x_c$. This leads to a significant decrease of the surface temperature at $x = 0$ and the formation of an alternative „weak“ area of the conductive material in the inner layers, where a local temperature maximum occurs. For shallow modified layers (at values of $x_c < 10\,\mu\mathrm{m}$, shown in the box to Fig. 7 on the left), a significant influence on the formation of the radial temperature distribution in the vicinity of the maximum is exerted by the process of heat exchange with the surface, which leads to a particularly rapid increase in the threshold field. In the future, the surface temperature turns out to be lower than the temperature of the local maximum $T_{\max}$ in the depth of the material with an increase in the parameter x_c to the value $x_{c,\max}$, and an increase in the threshold field is associated with a decrease of $T_{\max}$ due to its removal from the surface and the distribution of absorbed heat over an increasing volume.

The yield strength with the threshold value of the magnetic field is reached in the vicinity of the internal local

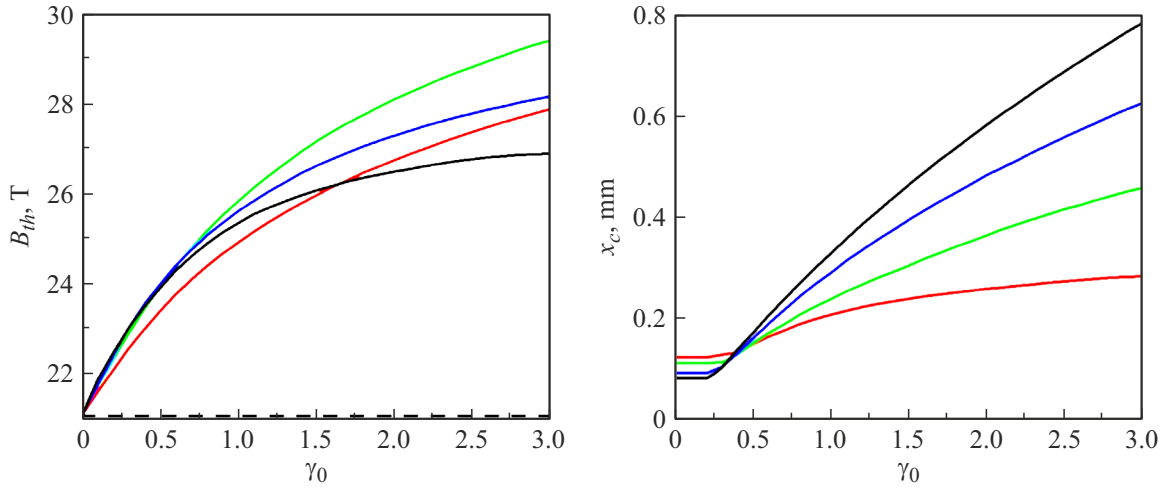

Figure 8. The maximum threshold field is $B_{th,\max}$ (left) and the corresponding thickness of the modified layer is $x_{c,\max}$ (right) depending on the „amplitude“ modifications γ_0. The line designations are the same as in Fig. 7.

maximum temperature in the range of values $x_c < x_{c,\max}$ for profiles with $N_\gamma > 1$. With an increase of the depth of the modified layer, the temperature decrease on the surface stops, and starting from $x_c = x_{c,\max}$, the „weak“ place returns to the working surface of the conductor at $x = 0$. This leads to the presence of a break point on the curves $B_{th}(x_c)$ at the maximum point at $N_\gamma > 1$. The most optimal depth of the modified layer $x_c = x_{c,\max}$ is characterized by the achievement of the yield threshold by stresses simultaneously at the point of the local maximum temperature in the depth of the material and on the working surface ($x = 0$). The values of temperature on the surface T_0 and in the local maximum $T_{\max}$ coincide in the plane geometry ($R_1 \to \infty$), i.e. $T_0 = T_{\max} = T_{plast,\infty}$ [15]. This, in particular, makes it possible to use an analytical estimate of critical heating (10) for a flat working surface for both homogeneous and surface-modified conductors. In cylindrical geometry optimal conditions are characterized by a higher temperature at the local maximum with finite R_1 than on the surface ($T_0 < T_{\max}$), which is associated, as noted above, with an additional source of stress growth when heating curved layers – is a term proportional to r^{-1} in (7). Therefore, in particular, the analytical estimate of the limit heating (15) loses its rigor for a curved modified surface. For an exponential profile with $N_\gamma = 1$, the return of the weak“ place from the depth to the surface with an increase in the parameter x_c occurs to the left of the maximum on the dependence $B_{th}(x_c)$, and the corresponding break point is less noticeable in Fig. 7.

An increase of the „amplitude“ γ_0 of the resistivity modification makes it possible to achieve higher values of the threshold field B_{th} as shown in Fig. 8. It is interesting to note here that with a decrease in the value of γ_0, the profile corresponding to the value of $N_\gamma = 2.3$ loses its advantages at amplitudes of $\gamma_0 < 0.5$, and is most effective for increasing the resistance of the conductive material, although with extremely minor differences in magnitude B_{th}, the resistivity profiles become sharper, up to a stepwise one ($N_\gamma \to \infty$). At the same time, the step profile becomes the most inefficient of those presented in Fig. 8 at high amplitudes of modification, starting from $\gamma_0 \approx 1.7$. The dependencies of the maximum coordinate of the threshold field $x_{c,\max}$ on the value of γ_0 for the four analyzed types of the modification profile are shown in Fig. 8 on the right. We see that an increase of the durability of the material with an increase in the amplitude of modification γ_0, as a rule, implies the need for the formation of deeper modified layers. The exception is the area of weak modifications at $\gamma_0 < 0.3$. Here, the optimal „depth“ of the modified layer $x_{c,\max}$ is stabilized at values from 85 μm for a stepped profile up to 125 μm for exponential profile due to the increased role of heat transfer at small values x_c.

Conclusion

As a result of the conducted study, the probability of destruction of a brittle conductive material in the form of a hollow cylinder under the action of a strong pulsed magnetic field with an induction of about 30 T in its internal cavity is analyzed. The geometry of the problem corresponds to the well-known actual problem of destruction of inductor systems — the inner surface of a solenoid or a magnetic flux concentrator in case of a generation of pulses of a strong magnetic field. The theoretical model takes into account the diffusion of the magnetic field, ohmic heating of the conductive material, its thermal conductivity and the mechanical stresses arising in it. The amplitude of the magnetic field at which the induced thermomechanical stresses in the material meet the Mises plasticity condition is used as a threshold field B_{th} separating the regions of safe (non-destructive) and dangerous fields. An analytical expression is obtained in case of a homogeneous material that allows

estimating with high accuracy the corresponding maximum heating temperature, which determines the achievement of a critical level of thermomechanical stresses.

Based on the analysis of the calculated values of the threshold field B_{th} , the influence of various parameters (magnetic pulse characteristics, elastic modules of the material, etc., etc.) on the resistance of the conductor in a pulsed magnetic field is investigated. It is shown that electrical circuits with relatively rapid attenuation of electromagnetic oscillations are preferred to increase the lifespan of the inductor system with characteristic attenuation time T_e less than the oscillation period T_s. This is explained by the fact that the main („working") half-period, which creates the main maximum of the magnetic field, is the first half-period at $t < T_s/2$, while subsequent electrical oscillations lead only to additional („parasitic") heating of the conductive material. The most significant characteristic of the material for the resistance of the inductor is the specific heat capacity. All other things being equal (first of all, with the same specific conductivity), it is preferable to use a conductor with a high value as an inductor material.

The possibility of increasing the resistance of a conductive material due to the formation of a modified surface layer in it with an increased value of the initial resistivity ρ_e is investigated in detail. Various profiles of the initial resistance from a smooth (exponential) profile $\rho_e(r)$ to the sharpest (stepwise) are considered. It is found that, the formation of a modified surface layer makes it possible to significantly increase the amplitude of the magnetic pulse field sustained by the material without destruction in comparison with a homogeneous material. In particular, it is possible to increase the threshold field B_{th} of the steel inductor at the most optimal shape and depth profile $\rho_e(r)$ by about 28% or from 21.1 to 27.1 T with the „amplitude" modification $\gamma_0 = 1.5$, i.e. when the resistivity on the surface is 2.5 times higher than the corresponding value in the depth of the material.

Funding

The study was funded by a grant from the RFBR and ROSATOM № 20-21-00050.

Conflict of interest

The authors declare that they have no conflict of interest.

References

[1] E.S. Ostropiko, S.G. Shops, S.I. Krivosheev. ZhTF, **92** (1), 174 (2022) (in Russian). DOI: 10.21883/JTF.2022.01.51868.247-21
[2] G.Sh. Boltachev, K.A. Nagayev, S.N. Paranin, A.V. Spirin, N.B. Volkov. *Magnetic Pulsed Compaction of Nanosized Powders* (Nova Science Publishers, Inc., N.Y.C., 2010)
[3] E.A. Olevsky, A.A. Bokov, G.Sh. Boltachev, N.B. Volkov, S.V. Zayats, A.M. Ilyina, A.A. Nozdrin, S.N. Paranin. Acta Mech., **224** (12), 3177 (2013). DOI: 10.1007/s00707-013-0939-6
[4] G.Sh. Boltachev, N.B. Volkov, S.N. Paranin, A.V. Spirin. Tech. Phys., **55** (6), 753 (2010). DOI: 10.1134/S1063784210060010
[5] E.L. Strizhakov, S.V. Neskromny, R.V. Merkulov. Svarka i diagnostika, **4**, 43 (2012) (in Russian).
[6] V.I. Krutikov, S.N., Paranin, D.S. Koleukh, V.V. Ivanov, A.V. Spirin, J.-G. Lee, M.-K. Lee, C.-K. Rhee. Izvestiya Vuzov. Fizika, **57** (11/3), 264 (2014) (in Russian).
[7] A.V. Spirin, G.Sh. Boltachev, V.I. Krutikov, S.N. Paranin, P.A. Russkikh, D.S. Koleukh. AIP Conf. Proc., **2174**, 020163 (2019). DOI: 10.1063/1.5134314
[8] S.I. Krivosheev, Yu.E. Adamian, D.I. Alekseev, S.G. Magazinov, L.V. Chernenkaya, V.V. Titkov. J. Phys. Conf., **1147**, 012033 (2019). DOI: 10.1088/1742-6596/1147/1/012033
[9] F. Herlach. *Strong and Ultrastrong Magnetic Fields and Their Applications* (Springer-Verlag, Berlin, 1985)
[10] S. Manson. *Temperaturnye napryazhenia i malotsiklovaya ustalost* (Mashinostroenie, M., 1974)
[11] V.V. Titkov. ZhTF, **59** (9), 72 (1989) (in Russian).
[12] V.V. Titkov. ZhTF, **61** (4), 54 (1991) (in Russian).
[13] I.M. Karpova, V.V. Titkov. ZhTF, **64** (7), 137 (1994) (in Russian).
[14] I.M. Karpova, V.V. Titkov. ZhTF, **65** (6), 54 (1995) (in Russian).
[15] P.A. Russkikh, G.Sh. Boltachev, S.N. Paranin, A.V. Kebets. IEEE Trans. Plasma Sci., **49** (9), 2463 (2021). DOI: 10.1109/TPS.2021.3092788
[16] A.V. Spirin, P.A. Russkikh, V.I. Krutikov, S.N. Paranin, D.S. Koleukh. *20th Int. Symp. on High-Current Electronics* (Tomsk, Russia, 2018), p. 148–153. DOI: 10.1109/ISHCE.2018.8521205
[17] I.M. Karpova, A.N. Semakhin, V.V. Titkov, G.A. Shneerson. *Analysis of Methods of Lowering Heating of and Thermal Stresses in the Coils in Nigh Magnetic Fields. Megagauss Magnetic Fields and Pulsed Power Systems* (Nova Science Publishers, N.Y.C., 1990)
[18] I.M. Karpova, V.V. Titkov. Elektrichestvo, **12**, 55 (1999) (in Russian).
[19] G.A. Shneerson, A.A. Parfentiev, V.V. Titkov, S.I. Krivosheev, A.D. Lagutkina, A.S. Nemov, A.P. Nenashev, S.A. Shimansky. Tech. Phys. Lett., **47**, 573 (2021). DOI: 10.1134/S1063785021060134
[20] A.V. Spirin, E.Y. Zaytsev, S.N. Paranin. IEEE Trans. Magn., **58** (6), 1 (2022). DOI: 10.1109/TMAG.2022.3165386
[21] G.A. Schneerson. *Fields and transients in the equipment of super-strong currents* (Energoatomizdat, M., 1992) (in Russian).
[22] G. Knopfel. *Super-strong pulsed magnetic fields* (Mir, M., 1972) (in Russian).
[23] O. Schnitzer. Phys. Plasmas, **21**, 082306 (2014). DOI: 10.1063/1.4892398
[24] R. Holland. IEEE Trans. Antennas Propag., **43** (7), 653 (1995). DOI: 10.1109/8.391135
[25] J.R. Brauer, I.D. Mayergoyz. IEEE Trans. Magn., **40** (2), 537 (2004). DOI: 10.1109/TMAG.2004.824591
[26] B. Tellini, M. Bologna, D. Pelliccia. IEEE Trans. Magn., **43** (3), 1112 (2005). DOI: 10.1109/TMAG.2004.841700

[27] Yu.E. Adam'yan, E.A. Vyrva, S.I. Krivosheev, V.V. Titkov. Tech. Phys., **58** (10), 1397 (2013). https://doi.org/10.1134/S1063784213100022
[28] S.E. Rosenthal, M.P. Desjarlais, R.B. Spielman, W.A. Stygar, J.R. Asay, M.R. Douglas, C.A. Hall, M.H. Frese, R.L. Morse, D.B. Reisman. IEEE Trans. Plasma Sci., **28** (5), 1427 (2000). DOI: 10.1109/27.901209
[29] S.F. Garanin, G.G. Ivanova, D.V. Karmishin, V.N. Sofronov. J. Appl. Mech. Tech. Phys., **46** (2), 153 (2005). DOI: 10.1007/PL00021891
[30] S.I. Krivosheev, V.S. Pomazov, G.A. Shneerson. Tech. Phys. Lett., **37** (9), 877 (2011). DOI: 10.1134/S1063785011090227
[31] S.I. Krivosheev, S.G. Magazinov, D.I. Alekseev. J. Phys. Conf., **946**, 012040 (2018). DOI: 10.1088/1742-6596/946/1/012040
[32] A.J. Mestel. Proc. Math. Phys. Eng. Sci., **405**, 49 (1986). DOI: 10.1098/rspa.1986.0040
[33] S.I. Krivosheev, S.G. Magazinov, G.A. Shneerson. Tech. Phys. Lett., **45** (2), 100 (2019). DOI: 10.1134/S1063785019020093
[34] A.V. Spirin, G.Sh. Boltachev, S.N. Paranin, V.I. Krutikov, D.S. Koleukh, P.A. Russkikh. Proceedings of EAPPC & BEAMS (Changsha, China, 2018), p. 172–176.
[35] L.D. Landau, E.M. Lifshitz. *Theory of Elasticity* (Pergamon Press, Oxford, 1993)
[36] L.I. Sedov. *Mechanics of Continuous Media 1 and 2* (World Scientific, Singapore, 1997)
[37] A.P. Babichev, N.A. Babushkina, A.M. Bratkovsky. *Tables of physical quantities* (Energoatomizdat, M., 1991) (in Russian).
[38] F. Heringhaus, H.-J. Schneider-Muntau, G. Gottstein. Mater. Sci. Eng. A, **347**, 9 (2002). DOI: 10.1016/S0921-5093(02)00590-7
[39] Q. Yuanshen, R. Lapovok, Yu. Estrin. J. Mater. Sci., **51**, 6860 (2016). DOI: 10.1007/s10853-016-9973-9
[40] P.A. Russkikh, G.Sh. Boltachev, S.N. Paranin. AIP Conf. Proc., **2113**, 030028 (2020). DOI: 10.1063/5.0032221
[41] A.R. Bryant. *The Intern. Conf. on Megagauss Magnetic Fields Generation by Explosives and Related Experiments Proc.* (Euroatom, Brussel, 1966), p. 183–191.
[42] G. Carslaw, D. Eger, *Teploprovodnost tverdykh tel* (Nauka, M., 1964) (in Russian).

Translated by A.Akhtyamov